Hindawi Publishing Corporation
Epilepsy Research and Treatment
Volume 2012, Article ID 736784, 10 pages
doi:10.1155/2012/736784

Clinical Study

Noninvasive Approach to Focal Cortical Dysplasias: Clinical, EEG, and Neuroimaging Features

Gustavo Seifer,[1,2] Alejandro Blenkmann,[1,2,3,4] Juan Pablo Princich,[1,2,4] Damián Consalvo,[1,2] Cristina Papayannis,[1,2] Carlos Muravchik,[3,5] and Silvia Kochen[1,2,4]

[1] *Epilepsy Laboratory, IBCN, "Prof. E. De Robertis", School of Medicine, University of Buenos Aires, Paraguay 2155, 1121 Buenos Aires, Argentina*
[2] *Epilepsy Section, Division of Neurology, Ramos Mejía Hospital, Urquiza 609, 1221 Buenos Aires, Argentina*
[3] *LEICI, School of Engineering, National University of La Plata, 48 y 116, 1900 La Plata, Argentina*
[4] *National Scientific and Technical Research Council (CONICET), Rivadavia 1917, 1033 Buenos Aires, Argentina*
[5] *Scientific and Technical Research Commission, 526 e/ 10 y 11, Buenos Aires, 1900 La Plata, Argentina*

Correspondence should be addressed to Gustavo Seifer, seifergustavo@yahoo.com.ar

Received 17 August 2011; Revised 10 November 2011; Accepted 21 November 2011

Academic Editor: Louis Lemieux

Purpose. The main purpose is to define more accurately the epileptogenic zone (EZ) with noninvasive methods in those patients with MRI diagnosis of focal cortical dysplasia (FCD) and epilepsy who are candidates of epilepsy surgery. *Methods*. Twenty patients were evaluated prospectively between 2007 and 2010 with comprehensive clinical evaluation, video-electroencephalography, diffusion tensor imaging (DTI), and high-resolution EEG to localize the equivalent current dipole (ECD). *Key Findings*. In 11 cases with white matter asymmetries in DTI the ECDs were located next to lesion on MRI with mean distance of 14.63 millimeters with topographical correlation with the EZ. *Significance*. We could establish a hypothesis of EZ based on Video-EEG, high-resolution EEG, ECD method, MRI, and DTI. These results are consistent with the hypothesis that the EZ in the FCD is complex and is often larger than visible lesion in MRI.

1. Introduction

Drug-resistant epilepsy is associated with malformations of cortical development (MCD) in 15–20% of adult cases and in more than 50% of pediatric patients [1–3]. MCD are a heterogeneous group of focal and diffuse anatomical derangements whose pathological features depend largely on the timing of the defect in the developmental process and to a lesser extent on its cause [4, 5]. Focal cortical dysplasia (FCD) is the most frequent type of MCD. Taylor et al. (1971) were the first to describe them as focal anomalies of cortical structure [6]. Numerous classifications of FCD have been proposed; a consensus clinic-pathological classification has been recently published [7]. However, it is widely recognized that existing classifications are unsatisfactory to define a prognosis [8, 9]. Furthermore, the etiology of these abnormalities is often uncertain and the mechanisms generating epilepsy are also unclear [10]. Several studies reported that FCD are intrinsically epileptogenic and most patients often present drug resistant epilepsy [11–16]. Some authors described the epileptogenic zone (EZ) as focal [17], while others suggest a more complex network extending beyond the lesion, an "epileptogenic network" [18]. Resective surgery is frequently a promising therapy in this population. However, the outcome following surgical treatment of these patients has been less successful than in other pathologies such as hippocampal sclerosis, even if the entire magnetic resonance images (MRIs) visible lesion is removed [19]. The surgical failure in these patients may be due to the difficulty in defining the epileptogenic zone, which can be more extensive involving apparently normal cortical areas in MRI [20]. The key for the success of surgical treatment is the accurate definition of the "epileptogenic zone" (EZ), the area of cortex that is indispensable for the generation of epileptic seizures and which removal or disconnection achieved seizure-free [21–24]. Today the

gold-standard method to define the EZ is the intracranial recording, an invasive procedure that increases morbidity and mortality. In addition, it demands an important amount of materials and human resources. These facts reduce the number of patients undergoing epilepsy surgery, which is below the number of cases for whom it is indicated. This situation is especially notorious in developing countries. In this scenario, noninvasive studies to define EZ are highly desirable [25]. The study of the EZ involves also the "irritative zone" (IZ), the area of cortex responsible for the scalp electroencephalography (EEG) interictal spikes (IISs). Both of these zones are also related to the onset zone of seizures [21, 22]. IIS neural sources can be located solving the so-called inverse problem with an equivalent current dipoles (ECDs) model. The ECD based on scalp EEG is the most often used model for noninvasively estimating the source of cerebral activity, specially to localize the origin of IIS activity [26–28]. The application of this model in patients with epilepsy and FCD was reported in using EEG [13, 22, 29] and using magnetoencephalography (MEG) [13, 14, 30, 31].

In this study we analyze a group of patients with epilepsy and FCD diagnosed by MRI. The main purpose is to obtain as much information as possible to delineate more accurately the hypothetical EZ with noninvasive methods in those patients who are candidates to epilepsy surgery. In these patients the EZ is suspected by ictal semiology and lesion seen in MRI. We applied ECD model treating to define more accurately the EZ and see the relative spatial distribution of ECDs as sources localized from single IIS, using 64-channel scalp EEG.

Twenty patients with diagnosis of epilepsy secondary to FCD according to MRI criteria [32, 33] were evaluated prospectively at the Epilepsy Center, Ramos Mejía Hospital between 2007 and 2010. At baseline all patients had resistant epilepsy, according to the new published criteria [34], with great impact on their quality of life. Two subjects improved seizure control after changes in antiepileptic drugs.

All included patients had a neurological examination, neuropsychological testing, routine MRI, and video-electroencephalography (V-EEG) with 32 channels, except those who became seizure-free ($n = 2$). Medical records were reviewed to identify (a) potential risk factors for the development of epilepsy, including prenatal trauma, perinatal bleed or infection, complicated delivery, childhood febrile seizures, head trauma, or family history of seizures, (b) ictal semiology according to the V-EEG and in the two subjects who became seizure free, the patient and relative's history were taking account, (c) sex, (d) age at seizure onset, (e) ictal semiology [35], and (f) response to treatment was considered in relation to seizure frequency [34].

All patients had conventional MRI criteria suggesting FCD including gyration anomalies, focal thickenings of the cortex, blurring of the grey-white matter junction, and abnormal cortical and subcortical signal intensity [32, 33]. The MRIs were evaluated retrospectively by two neurologists blind to the study. We assumed that FCDs are subtype II, according to the new ILAE classification [7]; since such kind of FCD is easier to detect by MRI, certain diagnosis it is possible only with histopathological data. The structure of white matter was evaluated by Diffusion Tensor Imaging (DTI) which is an MRI technique that can be used to indirectly evaluate the integrity of the axonal microenvironment by measuring the diffusion of water and its directionality in three dimensions [36]. Then, taking into account the findings of asymmetry of white matter structure in DTI, we selected a subset of patients for performing the ECD method.

The study was approved by the research ethics committee of the Ramos Mejía Hospital. Patients (and parents) gave their informed consent accepting the procedures in this study and the use of the information.

1.1. High-Resolution EEG and ECD. We recorded high-resolution EEG (HR-EEG) data from each patient with a 64-channel amplifier Bioscience EEG64 (Bioscience SRL, Argentina). Hardware filter frequency bandpass was 0.5–70 Hz (−3 dB) and sampling rate was set to 200 Hz. Harmonie 5.2 software (Stellate Systems Inc., Canada) was used to acquire data. Scalp electrodes were mounted on an Electro-Cap according to the international 10-10 system of electrode placement (including F9/10, FT9/10, T9/10, TP9/10, and P9/10) (Bio-Logic Systems Corp, USA). Recordings were referenced to average mastoidal electrodes. During acquisition sessions, patients were relaxed and asked to lie down with closed eyes for 3 hours in a sound attenuated and electrical shielded room. Before EEG recording started, we registered spatial coordinates of all electrodes and of three fiduciary landmarks (nasion, right and left tragi) with a three-dimension digitizer system PATRIOT (Polhemus, USA) and 3D Electrode Acquisition software developed by our group. Two position sensors were used, namely, a primary pen type sensor to acquire electrode and fiduciary points and a secondary sensor, fixed to the cap, as a position reference. After acquiring all electrode and fiducial positions, our software showed all the points on a 3D plot (Figure 1(a)).

1.2. Image Acquisition and Processing. In a second instance, patients were scanned with the same 1.5 T MRI unit (Intera, Philips Medical Systems, Best, The Netherlands). The acquired images were structural high-resolution 3D, T1-weighted spoiled gradient recovery volume (TR/TE/TI = 9.2/4.2/450 ms, matrix 256 × 256, bandwidth 31.2 kHz, field of view 256 mm × 256 mm, slice thickness 1 mm) with a final isotropic resolution of 1 mm. Depending on head sizes, approximately 160 slices in the axial plane were acquired and stored in DICOM format. Then, a 3D volume reconstruction, designated $T1_{Vol}$ from now on, was made of each patient head using MRIcron software (Chris Rorden's MRIcron, USA) in NIfTI format. A high-resolution mesh of 32768 triangles of the scalp surface was subsequently constructed from this volume using an iterative morphing algorithm in BrainVoyager2000 software (Brain Innovation, The Netherlands). In addition, all subjects were scanned with a 2D fluid attenuated inversion recovery (FLAIR) sequence (TR/TE/TI = 10,000/147/2200 ms, matrix 192 × 256, bandwidth 15.6 kHz, field of view 240 cm × 240 cm, slice thickness between 4 and 5 mm, no gap) in the coronal and

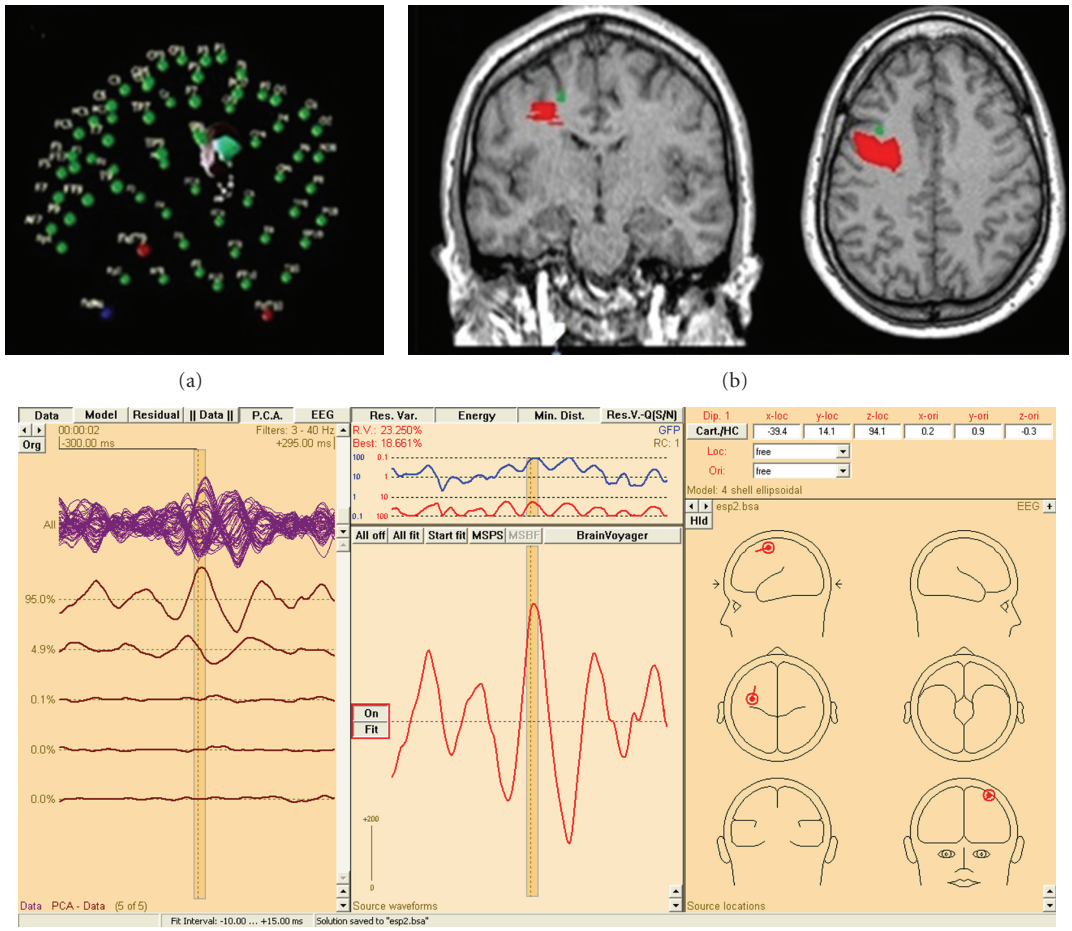

Figure 1: (a) 3D plot of electrodes and fiducial locations in a 3D virtual space in 3D electrode acquisition. (b) Left frontal FCD marked in Brain Voyager (red) overlaid on anatomical reconstruction with average dipole (green) near the lesion (distance: 4.47 mm). (c) An example of localization with BESA software.

axial planes. The integrity of white matter was also evaluated by means of DTI.

1.3. Lesion Marking and Processing. The more sensitive FLAIR sequence overlaid into the high-resolution T1 was mainly used to depict the shape and location of the lesion. Using a volume of interest (VOI) pen tool in MRIcron, an experienced neuroradiologist (J. P. Princich) marked the voxels corresponding to the suspected FCD on each slice (axial, sagittal, and coronal) (Figure 1(b)) according to previously established criteria [32, 37]. Thus, we obtained the set of voxels enclosing the anatomical lesion for each subject. These VOIs-denoted by $\text{Lesion}_{\text{Vol}}$, were then converted to NIfTI format in the same coordinate system as T1_{Vol}. Finally, using Matlab (The MathWorks, USA), a surface mesh describing the lesion border was constructed and its center of mass was calculated.

1.4. Registration of Electrodes and Fiducials with MRI. The electrode position coordinate system needs to be coregistered with T1_{Vol} and $\text{Lesion}_{\text{Vol}}$ space. For that purpose, we marked fiduciary landmarks on the scalp mesh surface and fitted the electrode coordinates to lay on the mesh, via a rigid body transformation in BrainVoyager2000. Fiduciary points were constrained to depart no further than 3 mm from the original position during the fitting procedure to avoid unfeasible electrode locations.

1.5. Selection of IIS. According to IFSECN criteria [38] we visually identified and selected IISs based on negative phase reversals on bipolar montages. The IISs were classified by morphology and frequency as single sharp waves or spikes, polyspikes, repetitive discharges lasting one or more seconds, or continuous discharges occupying more than 80% of the record. A sharp wave or spike was considered epileptiform if it had a sharp contour, duration of less than 200 msec and was clearly distinguished from ongoing background activity by its amplitude and duration [38]. When different types of IISs were found, they were collected in different groups. IISs were also classified according to spatial anatomical distribution as regional (maximum over a single lobe or

in two contiguous regions), multiregional (involving two or more regions in more than one lobe), or generalized. Afterwards, IISs were extracted in epochs of 400 ms (200 ms before and after the highest amplitude) and loaded into Matlab. Finally, signal-to-noise ratio (SNR) of every single IIS was calculated as the mean power of the spike interval over the mean power of the background activity. IISs with SNR smaller than 1.5 were discarded. We observe that no IIS data was averaged.

1.6. ECD Localization of IIS Neural Sources. IISs epochs were analyzed using Source Analysis module of Brain Electrical Source Analysis v5.1 (BESA) software (MEGIS Software GmbH, Germany). A high-pass filter at 3 Hz and a low-pass filter at 40 Hz were applied to all channels. Source localization for each single IIS was obtained solving the inverse problem with an ECD model of fixed location, fixed orientation, and time-varying amplitude. A four-shell ellipsoidal head model was used to solve the direct problem using the coregistered electrode position information. This model is utilized to compute the electric potential distribution on the scalp and to compare the values at the electrode locations with the actual measurements. Each of the layers in the model was assumed to have a constant value of homogeneous and isotropic conductivity relative to CSF.

2. Methods

2.1. Patients Selection. We assumed focal epileptogenic sources in these patients; therefore the source localization procedure was set to estimate a single focal source with one ECD. For each IIS the ECD was calculated fitting the zone of maximum energy (approximately ±6 ms from peak). When the first component of the principal component analysis (PCA) of the signal was larger than 90% the dipole was declared valid, and when it was less, the IIS was discarded.

2.2. Analysis of ECDs and FCD. Using the coregistration information, we overlaid in the same space ECDs, $T1_{Vol}$, and lesion surface mesh in Matlab (Figures 1(b) and 1(c)). We devised and calculated several different indicators with the objective of measuring the performance of source localization when comparing source with hypothetical epileptogenic lesion locations. First, from all ECDs of a single individual, an average dipole (AD) was defined, with the average location and orientation. Then, in terms of spatial distance to the MRI lesion, three indicators were measured: the distance from the AD to the lesion border (AD-L) and the mean of the distance from each ECD to the lesion border (ECD-L) and also the standard deviation from ECD-L (SD ECD-L). Individual ECD dispersion (Di) was calculated as the mean distance of each ECD to the AD. The smaller this value is the higher is the concentration of dipoles about AD.

2.3. Diffusion Tensor Imaging (DTI). DTI studies of the central nervous system rely on the phenomenon that water diffusion is anisotropic (i.e., highly ordered and tightly packed) in the normal white matter and are also the raw data to perform fibre tractography. Numerous model and clinical research studies have shown that DTI is sensitive to underlying abnormalities that are not apparent on conventional MR images [39, 40]. Fractional Anisotropy (FA) is an invariant rotational DTI index that can be quantified in each voxel with values ranging from zero (isotropic diffusion) to one (highly anisotropic diffusion). Reduced FA has been reported in the subcortical white matter underlying cortical abnormalities including FCD patients [40, 41], with anomalies extending even beyond the obvious cortical abnormality seen with conventional MRI [36, 42].

All patients were scanned consecutively since 2007 in the same MRI Unit at 1.5T (Intera, Philips Medical Systems, Best, Netherlands) using a six-channel head antenna with a (SENSE) "Sensitivity Encoding" factor of 2 for a single-shot diffusion-weighted echo planar imaging (TR/TE = 6,860/102 ms, matrix 128 × 128, bandwidth 95 KHz, field of view 22 × 22 cm^2), with *a b* value of (800 s/mm^2) applied sequentially in 32 non-collinear directions; at 60–70 axial slice positions one B0 image was acquired with no diffusion gradient applied at each slice location (2 mm thickness, no gap, and NSA: 3), with total scan time around 16-minute duration giving an in-plane reconstructed isotropic resolution of 2 mm. FA images of each subject were coregistered and resliced to their own high-resolution T1 3D and FLAIR images using SPM5 software from the Welcome Trust Centre for Neuroimaging (http://www.fil.ion.ucl.ac.uk/spm/). The evaluation of FA images overlaid to the T1 3D and FLAIR images was paired and assisted with the directional color maps projected on axial, sagital, and coronal planes using the DTI module of MedINRIA software (*MedINRIA v1.7*: Medical Image Navigation and Research Tool by INRIA).

A qualitative analysis was performed, by two independent examiners blinded to clinical and structural MRI findings. The asymmetries between regions were defined when both examiners agreed. The population was then divided in two groups, Group A: no asymmetries or representing mild or not clear focal or regional asymmetries between hemispheres on FA maps and Group B: with asymmetries, showing moderate-to-severe focal or regional asymmetries on FA maps. Both the Group A and Group B results were matched for age, sex, epilepsy duration, ictal semiology, and ECD (Figure 2).

3. Results

3.1. Clinical Data. We included 20 patients since 2007–2010. Mean age of our population was 25.9 years (9–46 years), 7 females, 13 males, they all had a negative family history of epilepsy, and only two patients had pathological neurological exam, both with mild contralateral paresis. Past medical history before epilepsy onset was relevant in 8 patients, five had febrile seizures (25%), one case a perinatal infection (5%), and two suffered of perinatal hypoxia/anoxia (10%). Three patients had mild-to-severe mental retardation.

Mean seizure onset age was 5.71 years (2 months–17 years) and the seizure frequency was 5.1 seizure per month (0–15). Two patients became seizure-free after adjusting antiepileptic drugs. Focal seizures were presented in the

Table 1: Mean clinical features.

Patient	Age (years)	Onset sz (years)	Personal history	Sz/month	MRI (FCD)	Initial sz semiology	DTI (FA maps)	Irritative zone (IIS)
1	15	5	No	5/month	Left frontal − medial aspect of superior gyrus	Tonic elevation of R arm	No asymmetries	
2	32	4	Prolonged labor	4/month	Left frontal − medial aspect of superior gyrus	Tonic posture of R arm	Moderate-to-severe asymmetries	ECDs
3	26	2	Febrile seizure	5/month	left parahippocampus	Auditory phenomena	No asymmetries	
4	30	10	Febril seizure	6/month	Right temporal − anterior middle gyrus	Mnemonic (deja vu) and dyscognitive phenomena	Moderate-to-severe asymmetries	ECDs
5	29	9	No	3/month	Right frontal − medial gyrus	Clonic of L arm	No asymmetries	ECDs
6	27	4	No	4/month	Right frontal (transmantle) − superior and middle gyrus	Hyperkinetic pedal movements	Moderate-to-severe asymmetries	ECDs
7	23	4	No	10/month	Right frontal (transmantle) perirolandic	Clonic of L arm	Moderate-to-severe asymmetries	ECDs
8	23	4	Febril seizure	6/month	Left frontoparietal (transmantle)	Clonic and somatosensory (tingling) phenomena of R arm	No asymmetries	
9	31	6 months	Perinatal infection	2/month	Right temporo-occipital	Mnemonic (deja vu) and dyscognitive phenomena	Moderate-to-severe asymmetries	ECDs
10	33	16	No	4/month	Right frontal (transmantle) middle gyrus	Tonic posture of L arm	Moderate-to-severe asymmetries	ECDs
11	5	5 months	Hypoxia	15/month	Right frontal anterior	Clonic of L arm	No asymmetries	
12	19	3	Hypoxia	8/month	Left parietal	Tonic posture of R arm	No asymmetries	
13	19	14	No	3/month	Right frontal (transmantle) - superior gyrus	L oculocephalic versive sz	Moderate-to-severe asymmetries	ECDs
14*	15	9 months	Febril seizure	Seizure free**	Right parietal + right HS	Mnemonic (deja vu) and dyscognitive phenomena	Moderate-to-severe asymmetries	ECDs
15	46	17	No	Seizure free**	Right frontal − middle gyrus	L hemiclonic movements	No asymmetries	
16	5	5	No	3/month	Right frontal − middle gyrus	Clonic of L arm with Jacksonian march	No asymmetries	
17*	23	3	No	14/month	Right frontal anterior	Tonic elevation of L arm	Moderate-to- severe asymmetries	ECDs
18	29	1	Febril seizure	4/month	Left frontal middle gyrus	Clonic of R arm		
19	12	11	No	3/month	Right frontal middle gyrus	Tonic posture of L arm	Moderate-to-severe asymmetries	ECDs
20	9	2 months	No	3/month	Right parietal + Left frontal cavernoma	L oculocephalic versive sz	No asymmetries	

R: right, L: left ISS: interictal spikes ECD: equivalent current dipoles FA maps: fractional anisotropy maps.
*Epilepsy surgery treatment.
**Improved seizure control after changes in antiepileptic drugs.

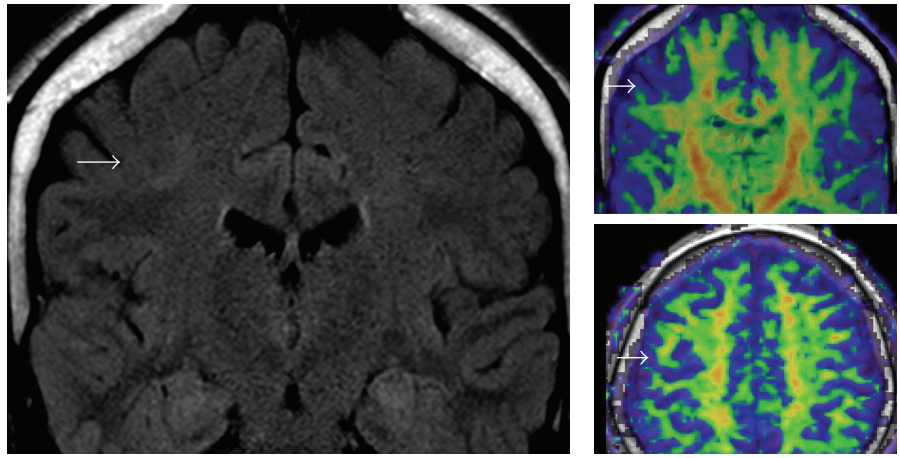

(a) (b)

Figure 2: Group "A" patient with right frontal middle gyrus FCD. (a) Coronal MRI FLAIR, (b) DTI anisotropy maps.

Table 2: Equivalent current dipoles (ECDs) localization results and measurements relative to focal cortical dysplasia (FCD).

Patient	ECDs	AD-L (mm)	Di (mm)	ECDs-L (mm)	SD ECD-L (mm)	Mean SNR	Mean GoF
1	4	4.63	12.96	7.55	10.37	2.8	77.95
2	34	3.97	13.04	13.29	8.14	4.2	86.23
3	4	3.1	27.47	10.99	6.45	2.59	67.48
4	7	13.57	12.32	16.57	7.52	3.74	83.86
5	9	25.09	16.78	28.17	13.99	3.24	86.05
6	5	1.41	18.49	9.46	4.74	3.97	77.21
7	10	22.9	14.22	25.56	12.98	5.67	74.33
8	12	57.44	14.93	59.53	9.74	2.81	79.48
9	12	19.44	7.23	20.89	3.03	5.45	89.01
10	8	4.72	17.29	6.27	9.22	5.21	64.9
11	3	4.66	28.85	20.96	12.8	2.09	66.53
Total	9.82	14.63	16.69	19.93	9	3.8	77.55

100% of our population. The ictal onset zone was topographically correlated with the FCD visible by MRI. The initial semiology was as follows: 7 subjects had focal clonic seizures, 6 patients had focal asymmetrical tonic seizures, 2 patients had contralateral versive oculocephalic seizures, 3 patients had dyscognitive phenomena with impairment of memory, speech, attention, and perception, and one patient had auditory phenomena as initial manifestation and another subject had hyperkinetic pedal movements. All patients presented a single seizure type. Seven patients (35%) had secondarily generalized seizures. In the two cases of seizure free, clinical semiology was assumed taking account that the story of the patient and family members committed to their care match. None of our patients had status epilepticus, epilepsy partialis continua, or reflex seizures (Table 1).

3.2. MRI. The frontal lobe was affected in 14 cases (70%). In 10 cases (50%) the dysplastic cortex was located on the medial aspect of the brain, and there were no cases affecting both the medial and the lateral surfaces. Three cases involve at least two lobes. Five cases (25%) have a transmantle characteristics, all of them involving the frontal lobe (Table 1).

3.2.1. DTI. Nine patients (45%) were classified into Group A (no asymmetries) in the FA maps. Eleven patients (55%) were included in Group B (with asymmetries) in the FA maps. in ten of these patients the areas of focal or regional, subcortical decreased FA were around the FCD exceeding the structural limits detected on T1/FLAIR sequences. Three patients had associated widespread areas of increased or decreased FA which extended beyond the subcortical regional area of FCD, usually including a different brain lobe.

3.2.2. EEG and ECD. In all cases the interictal EEG shows focal features. The most common pattern of interictal activity was stereotyped rhythmic, 4–10 Hz, of repetitive medium-voltage sharp waves or spikes lasting more than 1 second, present in 12 patients (60%). 16 patients (80%) had isolated, intermittent sharp waves or spikes. The electrical field of both EEG phenomena was correlated with the anatomical location of FCD seen in MRI. A scalp ictal recording was obtained in 18 cases (90%). The onset of the ictal discharge was characterized by low-voltage fast activity in 14 patients (70%) and rhythmic sharp waves or spikes in 4 cases (20%). Ictal activity was focal and coincided with FCD

location in 10 patients. The ictal activity of FCD located in medial surface in 8 patients (40%) tends to be more regional or even has bilateral features.

Eleven out of 20 underwent dipole localization technique (Table 2). In Table 2 we summarize the localization analysis for each patient. All dipoles had a signal-noise ratio greater than 2 and a goodness of fit greater than 60%. The average number of ECD per patient was 9.82 (3–34). The overall mean distance between a patient average dipole (AD) to lesion border was 14.63 millimeters (1.41–57.44) and in 6 cases (54%) it was less than 5 mm. Dispersion of ECD varied between 7 and 28 mm, with a mean of 16.69 mm. In all cases ADs were located outside the visible lesion.

Two patients of the series underwent epilepsy surgery after neurophysiological exploration: one patient with FCD IIB of the right frontal middle gyrus and the other case with FCD IIB located in the right frontal pole. Both cases are seizure free (Engel 1A). The remaining patients in the series are awaiting surgery, except two subjects who improved seizure control after changes in antiepileptic drugs.

4. Discussion

Our series of 20 patients with MRI diagnosis of FCD presented a relatively lower frequency of seizures in relation to other descriptions [43–46]. All patients, except two who became seizures free, have drug-resistant epilepsy with a great impact on quality of life. No cases of status epilepticus, epilepsia partialis continua, and reflex seizures were observed. A possible explanation for this better course of epilepsy is that, unlike the other series, our series include also two patients who became nonsurgical candidates after adjustment of antiepileptic drugs. Almost all patients began their seizure at early childhood. All patients presented focal seizures with clinical semiology concordant with lesional area seen on MRI. As mentioned by other authors, FCD is associated with a wide range of clinical presentations [47–49].

Analysis of IISs seems to be particularly important for accurately delineation of ZE and an eventual surgical treatment [50–52]. Bautista et al. [51] concluded that the presence of interictal epileptiform discharges extending beyond the area of resection correlates with poor surgical outcome in patients with extrahippocampal epilepsy. In contrast, patients with focal interictal epileptiform discharges included in surgical resection have good surgical outcomes. ECD is based on HR-EEG data and allows identifying the underlying source of a given potential distribution [53]. In the present study, the mean distance of dipoles to lesion border was 14.63 mm. The results are consistent with the idea that the EZ in FCD is often larger than visible lesion in MRI, involving perilesional "normal appearing" cortex [24, 54]. As described by other authors, areas of FCD with most signal changes on MRI are those with balloons cells, while the areas with dysmorphic or cytomegalic cells generate lower signal changes on FLAIR sequence [32, 33, 55]. Balloon cells are electrically silent while dysmorphic and cytomegalic cells are believed to be the responsible for interictal and ictal discharges [10, 55–59]. Our findings reinforce the view that irritative zone, which can be larger than the actual EZ, in these cases exceeds the lesion visible by MRI and may be organized as networks beyond the borders of the lesion, or to more remote zones [18, 60, 61]. Many studies report, when complete resection of MRI visible lesion, over a 50–75% seizure-free rate is achieved [62], supporting the idea of intrinsic epileptogenicity [10, 15, 57, 63], but still leaves 25–50% of patients with seizures [60, 64, 65] this suggesting that EZ was not contained within the lesion in those cases. In all cases, identified ECD could be correlated with hypothesis of EZ, by ictal semiology, imaging appearance of FCD on MRI, and visual analysis of topography of paroxysmal activity in EEG. However we assume, as other authors have done, that the EZ is complex and may extend in some cases, beyond the limits of the lesion visible on MRI involving "normal appearing" perilesional cortex [17, 18, 51, 52, 54, 66, 67]. The importance of these findings is that the complete surgical removal of the FCD, the parts visible and nonvisible in MRI, is the main predictive of good outcome after surgery. Larger studies using ECD are needed as a complementary technique for delineating the EZ more precisely and planning less invasive neurophysiological exploration.

Qualitative inspection of DTI is commonly used in clinical practice and FA maps are applied in different research protocols to assess the integrity of white matter microstructure; reduced FA was associated with several pathologic conditions and not exclusively related to FCD. It could be a sensitive technique readily available for clinicians for in vivo assessment of white matter in FCD patients despite the limitations of visual subjective evaluation. To date, the existing DTI statistical methods for group analysis have several limitations [68]. According to previous publications [42], we have found areas of moderate or severe interhemispheric asymmetries associated to visible FCD lesion and also found more marked changes that extend beyond the lesion. These findings might represent imaging evidence of abnormal white matter around and beyond the MRI visible FCD. These findings could explain the complexity of definition of EZ in these cases and, perhaps, the pattern of spread observed in EEG [69–71].

A further step in this analysis is to correlate ECD, EZ, and MRI lesion with postsurgical evolution.

5. Conclusions

The anatomo-electroclinical profile of these patients is heterogeneous. In those cases with white matter asymmetries the mean distance of ECD to lesion visible in conventional MRI was 14.63 mm. This may reflect that the lesion or cortex areas nearby the lesion are also epileptogenic. These results are consistent with the view that the irritative zone in these cases exceed the lesion visible by MRI and the EZ may be organized as networks beyond the borders of the lesion or to more remote zones. With the ECD method we attempt to delineate more accurately the EZ, with the idea of limiting a possible neurophysiological exploration and, therefore, the associated morbidity. DTI is a promising new tool that can reveal structural white matter abnormalities.

A less invasive algorithm can be used to assess patients that are candidates to surgery, trying to reduce the extension of invasive studies and improving even further the profile of morbidity.

However, more studies assessing the suitability of all these techniques are needed to corroborate their better predictive value and its usefulness in these complex patients.

Ethical Approval

The authors confirm that they have read the journal's position on issues involved in ethical publication and affirm that this report is consistent with those guidelines.

Conflict of Interests

None of the authors has any conflict of interest to disclose.

References

[1] A. A. Raymond, D. R. Fish, S. M. Sisodiya, N. Alsanjari, J. M. Stevens, and S. D. Shorvon, "Abnormalities of gyration, heterotopias, tuberous sclerosis, focal cortical dysplasia, microdysgenesis, dysembryoplastic neuroepithelial tumour and dysgenesis of the archicortex in epilepsy. Clinical, EEG and neuroimaging features in 100 adult patients," *Brain*, vol. 118, no. 3, pp. 629–660, 1995.

[2] R. Kuzniecky, A. Murro, D. King et al., "Magnetic resonance imaging in childhood intractable partial epilepsies: pathologic correlations," *Neurology*, vol. 43, no. 4, pp. 681–687, 1993.

[3] A. J. Barkovich, R. I. Kuzniecky, G. D. Jackson, R. Guerrini, and W. B. Dobyns, "A developmental and genetic classification for malformations of cortical development," *Neurology*, vol. 65, no. 12, pp. 1873–1887, 2005.

[4] M. Marín-Padilla, "Developmental neuropathology and impact of perinatal brain damage. III: gray matter lesions of the neocortex," *Journal of Neuropathology and Experimental Neurology*, vol. 58, no. 5, pp. 407–429, 1999.

[5] P. Krsek, T. Pieper, A. Karlmeier et al., "Different presurgical characteristics and seizure outcomes in children with focal cortical dysplasia type I or II," *Epilepsia*, vol. 50, no. 1, pp. 125–137, 2009.

[6] D. C. Taylor, M. A. Falconer, C. J. Bruton, and J. A. Corsellis, "Focal dysplasia of the cerebral cortex in epilepsy," *Journal of Neurology Neurosurgery and Psychiatry*, vol. 34, no. 4, pp. 369–387, 1971.

[7] I. Blümcke, M. Thom, E. Aronica et al., "The clinicopathologic spectrum of focal cortical dysplasias: a consensus classification proposed by an ad hoc Task Force of the ILAE Diagnostic Methods Commission," *Epilepsia*, vol. 52, no. 1, pp. 158–174, 2011.

[8] A. Palmini, I. Najm, G. Avanzini et al., "Terminology and classification of the cortical dysplasias," *Neurology*, vol. 62, supplement 1, no. 6, pp. S2–S8, 2004.

[9] R. Spreafico and I. Blümcke, "Focal Cortical Dysplasias: clinical implication of neuropathological classification systems," *Acta Neuropathologica*, vol. 120, no. 3, pp. 359–367, 2010.

[10] C. Cepeda, V. M. André, M. S. Levine et al., "Epileptogenesis in pediatric cortical dysplasia: the dysmature cerebral developmental hypothesis," *Epilepsy and Behavior*, vol. 9, no. 2, pp. 219–235, 2006.

[11] D. Mattia, A. Olivier, and M. Avoli, "Seizure-like discharges recorded in human dysplastic neocortex maintained in vitro," *Neurology*, vol. 45, no. 7, pp. 1391–1395, 1995.

[12] T. Morioka, S. Nishio, H. Ishibashi et al., "Intrinsic epileptogenicity of focal cortical dysplasia as revealed by magnetoencephalography and electrocorticography," *Epilepsy Research*, vol. 33, no. 2-3, pp. 177–187, 1999.

[13] T. Bast, O. Oezkan, S. Rona et al., "EEG and MEG source analysis of single and averaged interictal spikes reveals intrinsic epileptogenicity in focal cortical dysplasia," *Epilepsia*, vol. 45, no. 6, pp. 621–631, 2004.

[14] E. Widjaja, H. Otsubo, C. Raybaud et al., "Characteristics of MEG and MRI between Taylor's focal cortical dysplasia (type II) and other cortical dysplasia: surgical outcome after complete resection of MEG spike source and MR lesion in pediatric cortical dysplasia," *Epilepsy Research*, vol. 82, no. 2-3, pp. 147–155, 2008.

[15] A. Palmini, A. Gambardella, F. Andermann et al., "Intrinsic epileptogenicity of human dysplastic cortex as suggested by corticography and surgical results," *Annals of Neurology*, vol. 37, no. 4, pp. 476–487, 1995.

[16] A. Palmini, "Electrophysiology of the focal cortical dysplasias," *Epilepsia*, vol. 51, supplement 1, pp. 23–26, 2010.

[17] F. Chassoux, B. Devaux, E. Landré et al., "Stereoelectroencephalography in focal cortical dysplasia. A 3D approach to delineating the dysplastic cortex," *Brain*, vol. 123, no. 8, pp. 1733–1751, 2000.

[18] S. Aubert, F. Wendling, J. Regis et al., "Local and remote epileptogenicity in focal cortical dysplasias and neurodevelopmental tumours," *Brain*, vol. 132, no. 11, pp. 3072–3086, 2009.

[19] J. T. Lerner, N. Salamon, J. S. Hauptman et al., "Assessment and surgical outcomes for mild type i and severe type II cortical dysplasia: a critical review and the UCLA experience," *Epilepsia*, vol. 50, no. 6, pp. 1310–1335, 2009.

[20] P. Widdess-Walsh, B. Diehl, and I. Najm, "Neuroimaging of focal cortical dysplasia," *Journal of Neuroimaging*, vol. 16, no. 3, pp. 185–196, 2006.

[21] H. O. Lüders, I. Najm, D. Nair, P. Widdess-Walsh, and W. Bingman, "The epileptogenic zone: general principles," *Epileptic Disorders*, vol. 8, supplement 2, pp. S1–S9, 2006.

[22] P. Chauvel et al., "The "epileptogenic zone" in humans: representation of intercritical events by spatio-temporal maps," *Revista de Neurología*, vol. 143, no. 5, pp. 443–450, 1987.

[23] F. Rosenow and H. Lüders, "Presurgical evaluation of epilepsy," *Brain*, vol. 124, no. 9, pp. 1683–1700, 2001.

[24] J. S. Ebersole, "Defining epileptogenic foci: past, present, future," *Journal of Clinical Neurophysiology*, vol. 14, no. 6, pp. 470–483, 1997.

[25] K. Radhakrishnan, "Challenges in the management of epilepsy in resource-poor countries," *Nature Reviews Neurology*, vol. 5, no. 6, pp. 323–330, 2009.

[26] C. M. Michel, M. M. Murray, G. Lantz, S. Gonzalez, L. Spinelli, and R. Grave De Peralta, "EEG source imaging," *Clinical Neurophysiology*, vol. 115, no. 10, pp. 2195–2222, 2004.

[27] J. S. Ebersole and S. Hawes-Ebersole, "Clinical application of dipole models in the localization of epileptiform activity," *Journal of Clinical Neurophysiology*, vol. 24, no. 2, pp. 120–129, 2007.

[28] C. Plummer, A. S. Harvey, and M. Cook, "EEG source localization in focal epilepsy: where are we now?" *Epilepsia*, vol. 49, no. 2, pp. 201–218, 2008.

[29] M. Gavaret, A. Trébuchon, F. Bartolomei et al., "Source localization of scalp-EEG interictal spikes in posterior cortex epilepsies investigated by HR-EEG and SEEG," *Epilepsia*, vol. 50, no. 2, pp. 276–289, 2009.

[30] H. Otsubo, A. Ochi, I. Elliott et al., "MEG predicts epileptic zone in lesional extrahippocampal epilepsy: 12 Pediatric surgery cases," *Epilepsia*, vol. 42, no. 12, pp. 1523–1530, 2001.

[31] R. Ramachandrannair, H. Otsubo, M. M. Shroff et al., "MEG predicts outcome following surgery for intractable epilepsy in children with normal or nonfocal MRI findings," *Epilepsia*, vol. 48, no. 1, pp. 149–157, 2007.

[32] A. James Barkovich and R. I. Kuzniecky, "Neuroimaging of focal malformations of cortical development," *Journal of Clinical Neurophysiology*, vol. 13, no. 6, pp. 481–494, 1996.

[33] A. J. Barkovich, R. I. Kuzniecky, A. W. Bollen, and P. E. Grant, "Focal transmantle dysplasia: a specific malformation of cortical development," *Neurology*, vol. 49, no. 4, pp. 1148–1152, 1997.

[34] P. Kwan, A. Arzimanoglou, A. T. Berg et al., "Definition of drug resistant epilepsy: consensus proposal by the ad hoc Task Force of the ILAE Commission on Therapeutic Strategies," *Epilepsia*, vol. 51, no. 6, pp. 1069–1077, 2010.

[35] W. T. Blume, H. O. Lüders, E. Mizrahi, C. Tassinari, W. Van Emde Boas, and J. Engel, "Glossary of descriptive terminology for ictal semiology: report of the ILAE Task Force on classification and terminology," *Epilepsia*, vol. 42, no. 9, pp. 1212–1218, 2001.

[36] A. D. de la Roque, C. Oppenheim, F. Chassoux et al., "Diffusion tensor imaging of partial intractable epilepsy," *European Radiology*, vol. 15, no. 2, pp. 279–285, 2005.

[37] N. Colombo, N. Salamon, C. Raybaud, Ç. Özkara, and A. J. Barkovich, "Imaging of malformations of cortical development," *Epileptic Disorders*, vol. 11, no. 3, pp. 194–205, 2009.

[38] "A glossary of terms most commonly used by clinical electroencephalographers," *Electroencephalography and Clinical Neurophysiology*, vol. 37, no. 5, pp. 538–48, 1974.

[39] C. C. Lim, H. Yin, N. K. Loh, V. G. E. Chua, F. Hui, and A. J. Barkovich, "Malformations of cortical development: high-resolution MR and diffusion tensor imaging of fiber tracts at 3T," *American Journal of Neuroradiology*, vol. 26, no. 1, pp. 61–64, 2005.

[40] S. K. Lee, D. I. Kim, S. Mori et al., "Diffusion tensor MRI visualizes decreased subcortical fiber connectivity in focal cortical dysplasia," *NeuroImage*, vol. 22, no. 4, pp. 1826–1829, 2004.

[41] E. Widjaja, G. Simao, S. Z. Mahmoodabadi et al., "Diffusion tensor imaging identifies changes in normal-appearing white matter within the epileptogenic zone in tuberous sclerosis complex," *Epilepsy Research*, vol. 89, no. 2-3, pp. 246–253, 2010.

[42] S. H. Eriksson, F. J. Rugg-Gunn, M. R. Symms, G. J. Barker, and J. S. Duncan, "Diffusion tensor imaging in patients with epilepsy and malformations of cortical development," *Brain*, vol. 124, no. 3, pp. 617–626, 2001.

[43] E. Wyllie, "Surgical treatment of epilepsy in children," *Pediatric Neurology*, vol. 19, no. 3, pp. 179–188, 1998.

[44] F. Andermann, "Cortical dysplasias and epilepsy: a review of the architectonic, clinical, and seizure patterns," *Advances in neurology*, vol. 84, pp. 479–496, 2000.

[45] N. Colombo, L. Tassi, C. Galli et al., "Focal cortical dysplasias: MR imaging, histopathologic, and clinical correlations in surgically treated patients with epilepsy," *American Journal of Neuroradiology*, vol. 24, no. 4, pp. 724–733, 2003.

[46] J. A. French, "Refractory epilepsy: clinical overview," *Epilepsia*, vol. 48, supplement 1, pp. 3–7, 2007.

[47] H. Otsubo, P. A. Hwang, V. Jay et al., "Focal cortical dysplasia in children with localization-related epilepsy: EEG, MRI, and SPECT findings," *Pediatric Neurology*, vol. 9, no. 2, pp. 101–107, 1993.

[48] S. Fauser, H. J. Huppertz, T. Bast et al., "Clinical characteristics in focal cortical dysplasia: a retrospective evaluation in a series of 120 patients," *Brain*, vol. 129, no. 7, pp. 1907–1916, 2006.

[49] J. F. Bautista, N. Foldvary-Schaefer, W. E. Bingaman, and H. O. Lüders, "Focal cortical dysplasia and intractable epilepsy in adults: clinical, EEG, imaging, and surgical features," *Epilepsy Research*, vol. 55, no. 1-2, pp. 131–136, 2003.

[50] A. Gambardella, A. Palmini, F. Andermann et al., "Usefulness of focal rhythmic discharges on scalp EEG of patients with focal cortical dysplasia and intractable epilepsy," *Electroencephalography and Clinical Neurophysiology*, vol. 98, no. 4, pp. 243–249, 1996.

[51] R. E. Bautista, M. A. Cobbs, D. D. Spencer, and S. S. Spencer, "Prediction of surgical outcome by interictal epileptiform abnormalities during intracranial EEG monitoring in patients with extrahippocampal seizures," *Epilepsia*, vol. 40, no. 7, pp. 880–890, 1999.

[52] A. Rassi-Neto, F. P. Ferraz, C. R. Campos, and F. M. Braga, "Patients with epileptic seizures and cerebral lesions who underwent lesionectomy restricted to or associated with the adjacent irritative area," *Epilepsia*, vol. 40, no. 7, pp. 856–864, 1999.

[53] S. Vulliemoz, L. Lemieux, J. Daunizeau, C. M. Michel, and J. S. Duncan, "The combination of EEG source imaging and EEG-correlated functional MRI to map epileptic networks," *Epilepsia*, vol. 51, no. 4, pp. 491–505, 2010.

[54] M. Wong, "Mechanisms of epileptogenesis in tuberous sclerosis complex and related malformations of cortical development with abnormal glioneuronal proliferation," *Epilepsia*, vol. 49, no. 1, pp. 8–21, 2008.

[55] G. W. Mathern, M. Andres, N. Salamon et al., "A hypothesis regarding the pathogenesis and epileptogenesis of pediatric cortical dysplasia and hemimegalencephaly based on MRI cerebral volumes and NeuN cortical cell densities," *Epilepsia*, vol. 48, supplement 5, pp. 74–78, 2007.

[56] F. Rosenow, H. O. Lüders, D. S. Dinner et al., "Histopathological correlates of epileptogenicity as expressed by electrocorticographic spiking and seizure frequency," *Epilepsia*, vol. 39, no. 8, pp. 850–856, 1998.

[57] K. Boonyapisit, I. Najm, G. Klem et al., "Epileptogenicity of focal malformations due to abnormal cortical development: direct electrocorticographic-histopathologic correlations," *Epilepsia*, vol. 44, no. 1, pp. 69–76, 2003.

[58] C. Cepeda, V. M. André, N. Wu et al., "Immature neurons and GABA networks may contribute to epileptogenesis in pediatric cortical dysplasia," *Epilepsia*, vol. 48, supplement 5, pp. 79–85, 2007.

[59] S. Francione, L. Nobili, F. Cardinale, A. Citterio, C. Galli, and L. Tassi, "Intra-lesional stereo-EEG activity in Taylor's focal cortical dysplasia," *Epileptic Disorders*, vol. 5, supplement 2, pp. S105–S114, 2003.

[60] L. Tassi, N. Colombo, R. Garbelli et al., "Focal cortical dysplasia: neuropathological subtypes, EEG, neuroimaging and surgical outcome," *Brain*, vol. 125, no. 8, pp. 1719–1732, 2002.

[61] L. Tassi, R. Garbelli, N. Colombo et al., "Type I focal cortical dysplasia: surgical outcome is related to histopathology," *Epileptic Disorders*, vol. 12, no. 3, pp. 181–191, 2010.

[62] E. Wyllie, Y. G. Comair, P. Kotagal, J. Bulacio, W. Bingaman, and P. Ruggieri, "Seizure outcome after epilepsy surgery in children and adolescents," *Annals of Neurology*, vol. 44, no. 5, pp. 740–748, 1998.

[63] J. D. Jirsch, E. Urrestarazu, P. LeVan, A. Olivier, F. Dubeau, and J. Gotman, "High-frequency oscillations during human focal seizures," *Brain*, vol. 129, no. 6, pp. 1593–1608, 2006.

[64] S. M. Sisodiya, "Surgery for malformations of cortical development causing epilepsy," *Brain*, vol. 123, no. 6, pp. 1075–1091, 2000.

[65] S. M. Sisodiya, "Surgery for focal cortical dysplasia," *Brain*, vol. 127, no. 11, pp. 2383–2384, 2004.

[66] E. Bertram, "The relevance of kindling for human epilepsy," *Epilepsia*, vol. 48, supplement 2, pp. 65–74, 2007.

[67] W. W. Sutherling, M. F. Levesque, P. H. Crandall, and D. S. Barth, "Localization of partial epilepsy using magnetic and electric measurements," *Epilepsia*, vol. 32, supplement 5, pp. S29–S40, 1991.

[68] P. J. Basser and D. K. Jones, "Diffusion-tensor MRI: theory, experimental design and data analysis—a technical review," *NMR in Biomedicine*, vol. 15, no. 7-8, pp. 456–467, 2002.

[69] D. W. Gross, A. Bastos, and C. Beaulieu, "Diffusion tensor imaging abnormalities in focal cortical dysplasia," *Canadian Journal of Neurological Sciences*, vol. 32, no. 4, pp. 477–482, 2005.

[70] B. Diehl, J. Tkach, Z. Piao et al., "Diffusion tensor imaging in patients with focal epilepsy due to cortical dysplasia in the temporo-occipital region: electro-clinico-pathological correlations," *Epilepsy Research*, vol. 90, no. 3, pp. 178–187, 2010.

[71] E. Widjaja, S. Z. Mahmoodabadi, H. Otsubo et al., "Subcortical alterations in tissue microstructure adjacent to focal cortical dysplasia: detection at diffusion-tensor MR imaging by using magnetoencephalographic dipole cluster localization," *Radiology*, vol. 251, no. 1, pp. 206–215, 2009.